A Personalized Lane-Changing Decision System Based on Improved Stackelberg Game and Traffic Flow Information

Tianluo Yao and Hui Jin

***Abstract*— A lane-changing decision system based on improved Stackelberg Game and traffic flow information is proposed. The system consists of three parts: Lane-Changing Demand Assessment, Lane-Changing Condition Assessment and Multi-Lane Game Model. In Lane-Changing Demand Assessment, a lane-changing demand function considering the urgency and potential of lane change is proposed and traffic flow information is used as input to make assessment more forward-looking. Lane-Changing Condition Assessment is developed to assess the feasibility of lane change. Existing game models determine players before the game starts, but in multi-lane scenarios, they cannot determine in advance who will participate in the game. Inclusion of unrelated players will cause the game to collapse. To solve the problem of multi-lane game, we propose a new mechanism to improve the Stackelberg Game, and develop Multi-Lane Game Model based on the improved Stackelberg Game. The mechanism changes the classical game structure and determines actual players halfway through the game, which expands the application scope of game theory in the field of lane change. Additionally, a classifier is designed to incorporate driving style into Multi-Lane Game Model for enhancing its personalization. To verify the performance of the lane-changing decision system, three experiments were carried out. The results indicate that by considering traffic flow information, the assessment of lane-changing demand becomes more forward-looking, thereby avoiding unnecessary lane changes. By comparing with human drivers, it's found that the decision-making of our system is more rational and reliable, mitigating the risks caused by the irrational decision-making of human drivers.**

***Index Terms*— Lane-changing decision, game theory, traffic flow, driving style.**

I. Introduction

AUTONOMUOS driving is a promising technology with great significance for improving traffic safety, efficiency, and ride comfort. In recent years, it has been developing toward intelligence and networking, and new technologies that integrate other disciplines are emerging rapidly. Lane change decesion-making is one of the key technologys to ensure the efficiency and safety of vehicles, and it also greatly affects traffic delays [1]. Depending on sensing system and internet of vehicle (IOV), vehicles can obtain real-time information of the surrounding environment [2]. As a result, many lane-changing decision systems based on different techniques have been developed. In this paper, a lane-changing decision system based on improved Stackelberg Game is proposed to realize lane change in multi-lane scenarios through multi-vehicle game and traffic flow information extraction.

Received 1 July 2024; revised 9 December 2024; accepted 14 January 2025. The Associate Editor for this article was R. Malekian. *(Corresponding author: Hui Jin.)*

The authors are with the Department of Mechanical Engineering, Beijing Institute of Technology, Beijing 100081, China (e-mail: yaotianluo@163.com; jinhui@bit.edu.cn).

Digital Object Identifier 10.1109/TITS.2025.3531921

A. Field Background

The mainstream methods of lane-changing decision-making are broadly divided into artificial rules and artificial intelligence (AI). Artificial rules originated from the Gipps model proposed by P. G. Gipps [3] in 1986. From 1996 to 2007, Yang et al. [4], Hidas [5], Toledo et al. [6], improved the method and broadened its application scenarios in succession and proposed microscopic traffic simulator model (MITSIM), simulation of the intelligent transport systems model (SITRAS) and integrated driving behavior model. Sun and Elefteriadou [7] integrated driving style into lane-changing model in 2012. Models based on artificial rules are not robust and only applicable in simple scenarios. With the development of artificial intelligence technology, more and more studies are biased towards AI methods. Scholars used a variety of machine learning algorithms to replace artificial rules such as Bayesian algorithm used by Hou [8]. In recent years, reinforcement learning seems to have become the mainstream of AI methods. The most classical model is the hidden Markov model(HMM) introduced by Toledo et al. [9] and its result showed a significant improvement. Ding et al. [10] established a lane-changing intention recognition model based on HMM. In addition, scholars also tried to introduce deep learning into reinforcement learning to improve the ability of parameter optimization and generalization of models [11], [12], [13], [14], [15], [16], [17], [18].

As one of the directions of AI, game theory has been applied to lane-changing decision and attracted significant attention in the field of intelligent transportation systems (ITS) [19]. Game theory itself is a discipline proposed to solve decision-making problems and has strong theoretical and mathematical foundation. Therefore, it is more targeted than other algorithms. Game theory rationally analyzes the influencing factors of decision-making and the nature of cooperation and competition between multiple vehicles, so players of a game can make the best decision after weighing the advantages and disadvantages. Additionally, game theory is better at making decisions than human beings because its players are perfectly

rational, and it can also be combined with predictive models such as [20] to improve performance. At present, game theory is preliminarily applied to lane-changing models to enhance intelligence, and the related studies are discussed below.

B. Related Studies

In a game model, the surrounding vehicles are viewed not only as moving obstacles but also as interactive objects, and decision-making of each vehicle is influenced by other vehicles. Therefore, a game model should take into account all the vehicles involved and not just focus on the lane-changing vehicle. The design of game models is gradually from simple to complex for adapting to various scenarios. Kita [21] designed a two-player static game model involving strategies of "changing lanes" and "giving up changing lanes", which is a basic form of game theory decision model and has some unrealistic assumptions. In response, Talebpour et al. [22] used Harsanyi transformation to establish an incomplete information game model, enhancing the practicability. Depending on sensing systems and IOV, vehicles can obtain real-time driving data of surrounding vehicles, enabling the realization of complete information games. Smirnov et al. [23] proposed a lane-changing model based on complete information dynamic game and sixteen sets of field test data demonstrated an 87.5% accuracy in lane change prediction. Sun [24] constructed a two-player static game model for scenarios where two vehicles on the same lane intend to drive into the same neighboring gap concurrently. Yoo and Langari proposed a lane-changing game model based on Stackelberg Game [25], which measures the payoffs by estimating collision risk. Pan et al. [26] constructed a two-player Stackelberg Game model for lane-changing decisions and integrated the game model into a model predictive controller to execute the lane-changing action. Yu et al. [27] proposed a multi-player Stackelberg Game model, which considered the multi-lane scenarios and solved the problem of two vehicles changing into the same spacing in a three-lane scenario. Guo et al. [28] proposed a method to decompose large-scale games into sub-games, reducing the complexity of game calculation in complex scenarios. Zhang et al. [29] and Deng et al. [30] introduced drivers' aggressive coefficients into the Bayesian Game Model. Drivers of different styles have various preferences in the game, and the game model is more acceptable and practical after considering driving style.

C. Gaps and Solutions

Based on the analysis of the related studies, there are still the following gaps:

1) Most game theory models are designed for two-lane scenarios and cannot make decisions in multi-lane scenarios. In fact, this problem is caused by the structure and mechanism of game theory. Before a game starts, the game model has to determine all players, their strategy sets and payoff functions. However, in a multi-lane scenario, the lane-changing vehicle cannot determine whether it plays the game with the vehicles on the left or on the right. If irrelevant players are included in the game, the game tree will collapse. Therefore, few studies have been conducted in multi-lane scenarios. Although some studies have considered multi-lane lane change, their methods are often realized indirectly by confusing multiple two-lane game models, and they have not improved the mechanism of the game theory itself.

2) When assessing the lane change demand, relying solely on information from the single preceding car fails to accurately reflect the real traffic flow state. This limitation often results in short-sighted decision-making.

3) Currently, few studies have considered personalization. While several studies do account for driving style, they often use offline recoginition models, that is, the driving style of all vehicles has been already known before the lane-changing experiment, which is obviously not of practical significance.

In view of the aforementioned gaps, this paper proposes a lane-changing decision system and makes contributions in the following aspects:

1) A multi-vehicle dynamic game mechanism is proposed to improve the classical Stackelberg Game theory and based on it, Multi-Lane Game Model is developed. This model can dynamically determine the actual players halfway through the game, resolving the dilemma mentioned above.

2) The system assesses lane-changing demand using 400-meter traffic flow information instead of the single vehicle's driving information. Additionally, a traffic anomaly coefficient is designed to compensate for the deficiency where the abnormal driving behaviors of individual vehicle may not be adequately captured through traffic flow information.

3) Driving style is integrated into the parameters of payoff functions in Multi-Lane Game Model. Participating in the game according to preferences and knowing the driving style of other vehicles and will enhance the personalization and rationality of decision-making in the game process. Additionally, an external real-time classifier is designed to provide real-time driving styles of all players to the lane-changing decision system during the game.

D. Paper Structure

In section II, as preparatory work, NGSIM dataset is preprocessed and a driving style classifier is designed. In section III, we propose the lane-changing decision system and introduce each part in detail. In section IV, three experiments are carried out to verify the performance of the system. In section V, a general summary of the paper is made.

II. Preparation: Data Preprocessing and Driving Style Classifier Design

A. Data Preprocessing

The dataset is sourced from the NGSIM database which is collected on the US-101 highway in Los Angeles, California, USA. The sampling period spans from 8:20 a.m. to 8:35 a.m., with a frequency of 10 Hz. In the preprocessing, we extract time-sequence driving data of all vehicles and remove the vehicles with data loss. In addition, SG filtering is performed to remove the noise of data and uses the least squares method to fit polynomials, with a convolution window size of 9 frames. Through analyzing and verifying, a larger value of the size will result in information loss, while a smaller one will lead

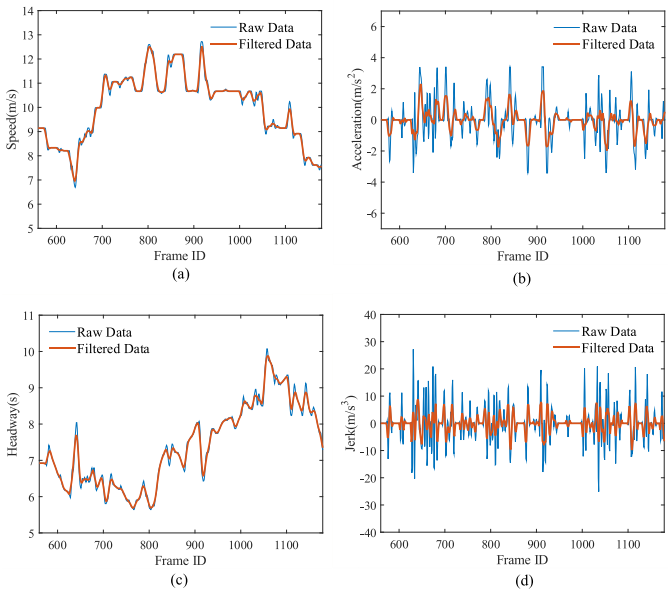

Fig. 1. Vehicle 101 time series features before and after filtering. (a) Speed (b) Acceleration (c) Headway (d) Jerk.

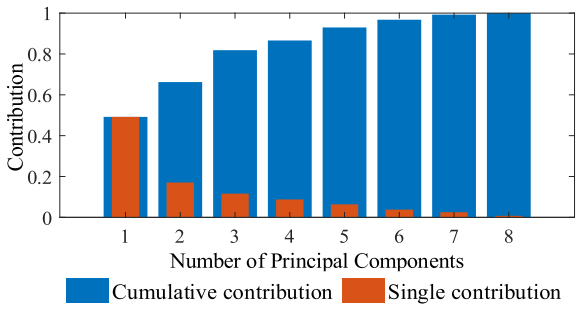

Fig. 2. Single contribution and cumulative contribution of principal components.

to less obvious noise cancellation. The vehicles numbered 11 to 1710 are selected from NGSIM preliminarily, and after preprocessing, 1124 vehicles among them are screened. Taking the vehicle numbered 101 as an example, the vehicle entered the sampling area at frame 560 and exited at frame 1205, and its driving data before and after filtering are shown in Fig. 1. Headway is defined as the distance between the front and the rear vehicles divided by the rear vehicle's speed.

As shown in Table I, eight statistical features are constructed based on relevant original features, and consequently, a feature matrix with a total size of 1124×8 is obtained. To eliminate the excessive contribution of features with large values, the data is normalized through (1). Besides, principal component analysis (PCA) is used to reduce the dimension of features and the contributions of principal components are shown in Fig. 2. The first three principal components are selected, cumulatively accounting for 81.85% of the total contribution.

$$e_{i,j-nor} = 2 * \frac{e_{i,j} - \min(E_i)}{\max(E_i) - \min(E_i)} - 1 \tag{1}$$

where $e_{i,j-nor}$ is normalized feature data, E_i is the i-th statistical feature vector, and $e_{i,j}$ is the j-th data of vector E_i.

TABLE I
(a) ORIGINAL FEATURES (b) STATISTICAL FEATURES

(a)

Original features	Unit
Instantaneous velocity	m/s
Instantaneous acceleration	m/s^2
Headway	s
Instantaneous jerk	m/s^3

(b)

Statistical features	Unit
Mean speed	m/s
Velocity standard deviation	m/s
Acceleration standard deviation	m/s^2
Mean acceleration	m/s^2
Reciprocal of mean headway	$1/s$
Reciprocal of median headway	$1/s$
Jerk standard deviation	m/s^3
Mean jerk	m/s^3

TABLE II
LABEL MATCHING RESULTS

	Aggressive	Normal	Calm
Label 1	0	83	439
Label 2	178	3	0
Label 3	81	302	38

B. Driving Style Classifier Design

Knowing the driving styles of surrounding vehicles is crucial for intelligent vehicles to make correct decisions in the game. Most studies adopt offline driving style recognition but this dosen't meet the real-time requirements of our system. Therefore, we design an online classifier to recognize driving style and its output is called "short-term style" because our classifier depends on the real-time sensor data rather than long-term historical data.

K-Means++ is used to provide labeled data for training the classifier below. We choose SSE (Sum of Squared Errors) as the loss function. Through several experiments, it's found that SSE of three clusters reach the "elbow point" [31], so driving style is divided into aggressive, normal and calm. Fig. 3 shows the clustering results and the change of loss. The clustering model generates three clusters in the dataset based on the features in Table I, and the number of labels for these three categories is shown in Table II. Based on matching results, label 1, 2, and 3 represent calm, aggressive, and normal driving styles, respectively.

$$SSE = \sum_{i=1}^{K}\sum_{j=1}^{N} r_{i,j} \cdot \left\| x_j - \mu_i \right\|_2^2, \quad r_{i,j} = \begin{cases} 0, & x_j \in C_i \\ 1, & x_j \notin C_i \end{cases} \tag{2}$$

where K and N is number of clusters and samples, x_j is feature vector of the j-th sample, and μ_i is cluster center of class i.

An online triple-classifier is designed and trained with the labeled dataset. The classifier consists of three support vector machines (SVM), and its structure is shown in Fig. 4.

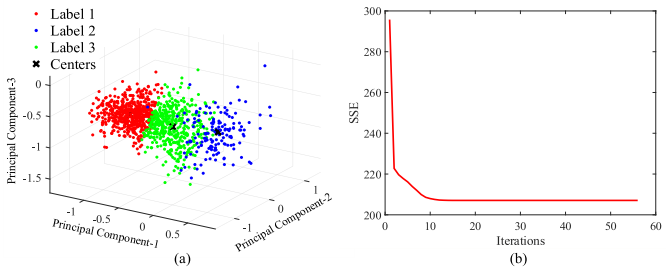

Fig. 3. Clustering results and objective function changes. (a) Clustering results (b) Loss function changes.

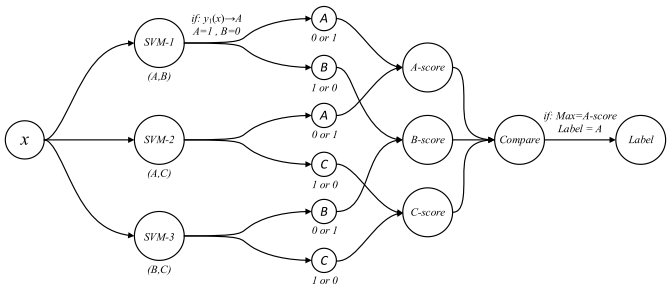

Fig. 4. Structure of online triple-classifier.

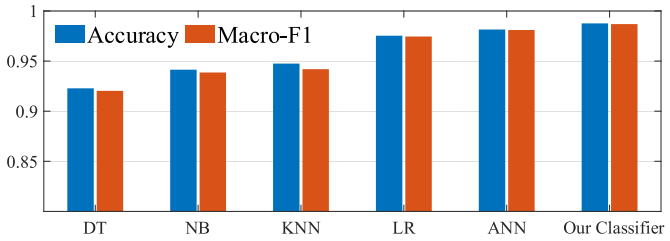

Fig. 5. Performance comparison of classifiers.

Assuming that A, B, and C are three categories. When smaple x is fed into the classifier, the three SVMs are responsible for classifying x in (A, B), (A, C) and (B, C), respectively. The values of selected categories are set to 1 and output to the next layer for accumulating. The category with the highest score will be output as the final label of sample x.

The dataset is divided into training and test sets by 800: 324, and verification set is selected by five-fold cross validation in each epoch. *accuracy* and *macro-F*1 score are selected as evaluation indicators, and introduced in (3) to (6). $precision_k$, $recall_k$ and $F1_k$ are the precision, recall rate and $F1$ score of class k. *macro-F*1 is the macro average of $F1$ scores. TP_k is the correct number of predictions for class k, and TN_k is that for classes other than k. FP_k is the number of the samples from other classes predicted incorrectly as class k, and FN_k is that from class k predicted incorrectly as other classes.

For horizontal comparisons, other classification models are test: K-nearest neighbors (KNN), Naïve-Bayes (NB), logistic regression (LR), decision tree (DT), and artificial neural network (ANN). In Fig. 5, LR, ANN, and our classifier all have good performance, among which our classifier achieves the highest *accuracy* and *macro-F*1 at 99.18% and 0.9869, and its detailed classification results are shown in Table III.

TABLE III
CLASSIFICATION RESULTS OF OUR CLASSIFIER

Class	TP	TN	FP	FN	Accuracy
Calm	142	179	3	0	99.07%
Normal	82	238	0	4	98.77%
Aggressive	96	227	1	0	99.69%
Mean Accuracy				99.18%	

$$accuracy = \frac{TP_k + TN_k}{TP_k + TN_k + FP_k + FN_k} \tag{3}$$

$$precision_k = \frac{TP_k}{TP_k + FP_k}, \quad recall_k = \frac{TP_k}{TP_k + FN_k} \tag{4}$$

$$F1_k = \frac{2 \cdot precision_k \cdot recall_k}{precision_k + recall_k} \tag{5}$$

$$macro - F1 = \sum_{k=1}^{3} F1_k \tag{6}$$

The classifier outputs short-term style labels of surrounding vehicles for each frame, but the style may frequently mutate. In order to ensure its stability, we combine the current output with the historical information, and transform discrete labels into a continuous driving style factor s. Its calculation formula is shown in (7), where S_n is the current output with values being -1, 0, and 1 corresponding to calm, normal, and aggressive. The influence of historical information decays exponentially. To ensure high stability, the attenuation coefficient is set to $\exp(-1/180)$, and the weight of historical information from 100 s ago is only 0.00387. s_n represents the driving style factor in the n-th time frame and its value range is $[-1, 1]$. The transition time from calm to normal should be the same as that from normal to calm, while the transition time from calm to aggressive should be twice as long. The threshold between normal and calm is set to -0.5, and similarly, that between normal and aggressive is set to 0.5. After calculation, it's found that if output jumps from -1 to 0, s will gradually increase from -1 to -0.5 after 12.5 seconds, which indicates that driving style has converted to normal, and if output jumps from -1 to 1, s will increase from -1 to 0.5 after 25 seconds. Therefore, compared to average division, the division method ensures that driving style can be smoothly transitioned and the status of three styles are equitable. If $s \in [-1, -0.5)$, the style is clam; if $s \in [-0.5, 0.5]$, it is normal; and if $s \in (0.5,1]$, it is aggressive.

$$S_n = \left(1 - e^{-1/180}\right) S_n + e^{-1/180} S_{n-1} \tag{7}$$

III. THE LANE-CHANGING DECISION SYSTEM

The system consists of three parts: Lane-Changing Demand Assessment, Lane-Changing Condition Assessment, and Multi-Lane Game Model. Lane-Changing Demand Assessment continuously assesses the demand for lane changes. When a demand is detected, Lane-Changing Condition Assessment will analyze the feasibility of the lane change. If the current situation meets the conditions, the vehicle will enter a

game decision-making process and collaborate with surrounding vehicles for the lane change through Multi-Lane Game Model.

A. Lane-Changing Demand Assessment

Lane-changing demand function R which is composed of the urgency function and potential function, is designed for assessment. The urgency of a lane change is determined by the difference between the average speed of the current traffic flow and the driver's expected speed, while the potential for a lane change is determined by the difference in average traffic flow speed between adjacent lanes and the current lane. Demands of lane changes are assessed based on traffic flow information within a 400-metre distance. Compared with the conventional assessment methods that only consider the kinematic characteristics of the single preceding vehicle, the method proposed in this paper focuses on the motion characteristics of the traffic flow, which is forward-looking and stable, and helps avoid frequent and invalid lane changes driven by local advantages.

In Fig. 6, *R-threshold* and *TIME-threshold* represent the maximum lane-changing demand value that can be tolerated and the longest time that the demand continues to exceed *R-threshold*, respectively. U_{L1} and U_{FA1} represent the leader's and follower A's payoffs when choosing Strategy Set-1. Note that they are originally $U_L(s_{L1}, s_{F1}^1)$ and $U_F^l(s_{L1}, s_{F1}^1)$ in the following formula deduction and are simplified in the figure. U_L^* and U_F^* are maximum payoffs of the leader and the follower. S_L^* and S_F^* are the optimal strategies of the leader and the corresponding follower.

1) Lane-Changing Urgency Function R_p: A driver's expected speed is defined as a variable related to his driving style. Fig. 7 shows average speed for each sample and it can be found that the average speed increases with the degree of aggressiveness. Expected speed of a certain driving style is calculated by averaging the speed of all samples of that style. Therefore, $v_{desire-c} = 7.60$ m/s, $v_{desire-n} = 9.29$ m/s, and $v_{desire-a} = 11.51$ m/s.

However, using traffic flow data to calculate demand values has a significant drawback: when a car in front is not cruising normally and its speed is significantly low due to certain operational problems, the rear vehicles are severely affected. This situation is referred to as an abnormal traffic state and cannot be promptly identified through traffic flow. To address this, an abnormal sensitivity factor ε is defined in (8). When ε is larger than the threshold ε', the vehicle is considered to be in an abnormal traffic state, and the representativeness of the traffic flow information decreases rapidly with time. From a practical perspective, the vehicles in the distance are moving rapidly but the preceding vehicle is unwilling to accelerate, resulting in a rapid decrease in the driver's expectations for the "long-term benefits" of the current lane over time, which is in line with human psychological process. Subsequently, the traffic anomaly coefficient ξ is defined in (9). The larger its value, the less reliable traffic flow information is, and using the speed of the current vehicle to calculate lane-changing demand is more reliable. When the vehicle exits the abnormal traffic state, the coefficient is reset to 0 and accumulated again.

$$\varepsilon = \frac{\bar{v} - v}{\bar{v}} \tag{8}$$

$$\xi = e^{-1/t_{\varepsilon \geq \varepsilon'}} \tag{9}$$

$$\Phi(x) = \begin{cases} x, & x > 0 \\ 0, & x \leq 0 \end{cases} \tag{10}$$

$$R_p = (1-\xi) \cdot \Phi\left(\frac{v_{desire} - \bar{v}}{v_{desire}}\right) + \xi \cdot \Phi\left(\frac{v_{desire} - v}{v_{desire}}\right) \tag{11}$$

where $\bar{v}$ is the average speed of the traffic flow in the current lane, v is the speed of the current vehicle, and $t_{\varepsilon > \varepsilon'}$ is the duration for which the vehicle has been in an abnormal traffic state.

2) Lane-Changing Potential Function R_q: Lane-changing potential function R_q is used to measure the improvement of driving experience. An adjacent lane has the potential for a lane change when its traffic flow speed is higher than that of the current lane. However, if the speed is excessively high and surpasses the expected speed, the driver's safety awareness decreases, thereby reducing the potential for a lane change. This phenomenon is referred to as overspeed loss in this paper. For simplicity, we defined $A(x)$ in (12), representing the difference between the overspeed loss of the current lane and the adjacent lane. A positive value indicates a reduction in overspeed loss, implying an improved driving experience after a lane change. The traffic anomaly coefficient of the current lane is introduced in (13), while that of the adjacent lane is introduced in (14). Finally, the lane-changing potential of an adjacent lane is R_{qi}. Among the left and right lanes, the one with greater potential will be chosen, and the lane-changing potential function R_q is (15).

$$A(x) = \alpha\left((1-\xi) \cdot \Phi\left(\frac{\bar{v}}{v_{desire}} - 1\right) + \xi \cdot \Phi\left(\frac{v}{v_{desire}} - 1\right) - \Phi\left(\frac{x - v_{desire}}{v_{desire}}\right)\right) \tag{12}$$

$$r(x) = \begin{cases} (1-\xi) \cdot \Phi\left(1 - \dfrac{\bar{v}}{v_{desire}}\right) + \xi \cdot \Phi\left(1 - \dfrac{v}{v_{desire}}\right) + A(x), & x \geq v_{desire} \\ (1-\xi) \cdot \Phi\left(\dfrac{x - \bar{v}}{v_{desire}}\right) + \xi \cdot \Phi\left(\dfrac{x - v}{v_{desire}}\right) + A(x), & x < v_{desire} \end{cases} \tag{13}$$

$$R_{qi} = (1-\xi_i) \cdot r(\bar{v}_i) + \xi_i \cdot r(v_i) \tag{14}$$

$$R_q = \max\left\{R_{q1}, R_{q2}\right\} \tag{15}$$

where α is overspeed loss coefficient, ξ is abnormal influence coefficient of the current lane, v is the current vehicle speed, $\bar{v}$ is the average speed of the traffic flow in the current lane, i is road number (the left and right road numbers are 1 and 2), v_i is the speed of the preceding vehicle on the adjacent lane, $\bar{v}_i$ is the average speed of the traffic flow in the adjacent lane, and ξ_i is the abnormal influence coefficient of the adjacent lane.

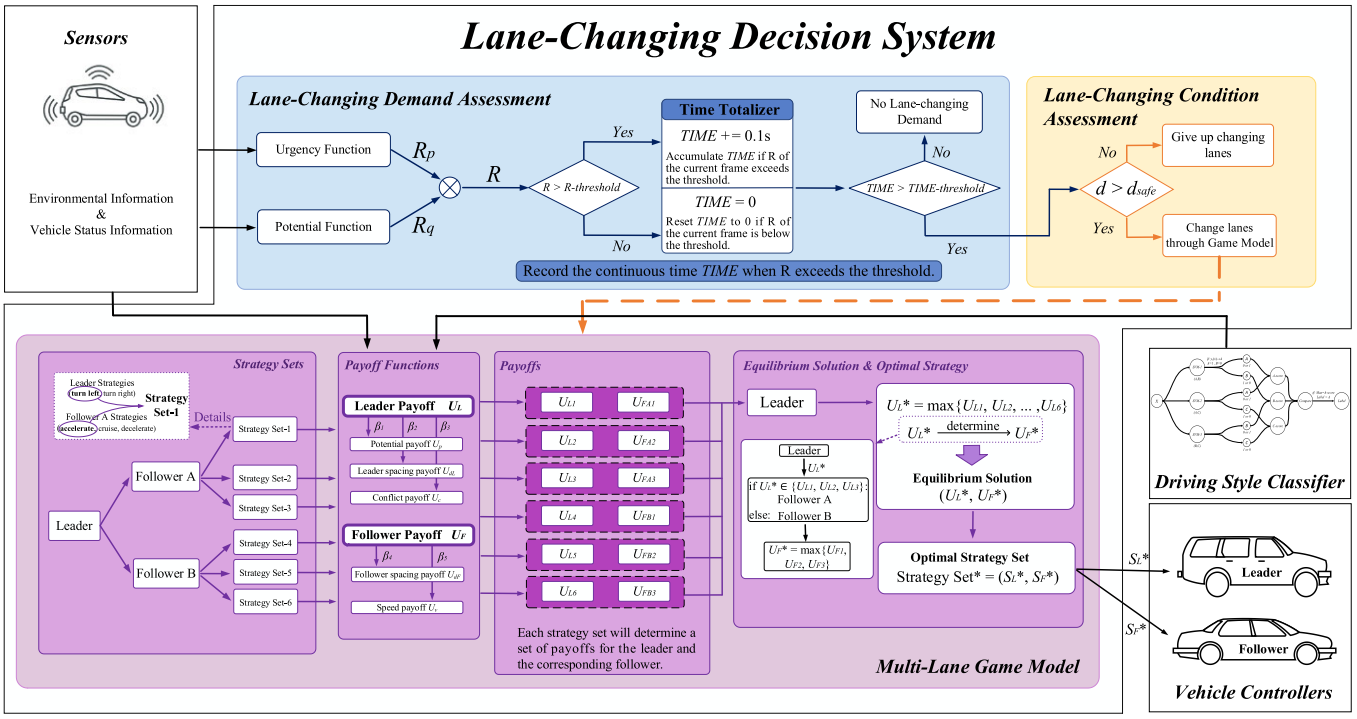

Fig. 6. Schematic diagram of the lane-changing decision system.

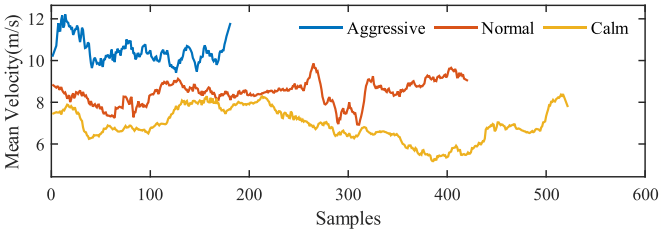

Fig. 7. Average speed of the 1124 samples covering the three driving styles.

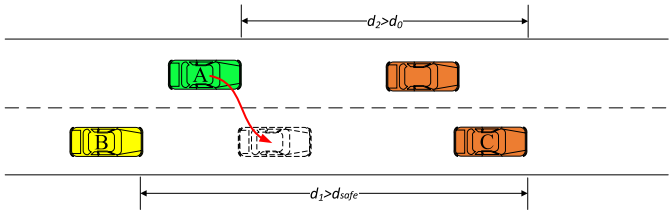

Fig. 8. Lane-changing condition assessment.

3) Lane-Changing Demand Function R: The lane-changing demand function combines the two indicators: lane-changing urgency and lane-changing potential. Lane-changing demand only exists when both indicators are non-zero, and the demand is positively correlated with the both indicators. Therefore, we set function R as the product of the two indicators.

$$R = R_p \cdot R_q \tag{16}$$

B. Lane-Changing Condition Assessment

To ensure the safety of lane change, we define the minimum lane-changing spacing as d_{safe}. When speed of the rear vehicle increases or aggressiveness of the lane-changing vehicle decreases, d_{safe} will increase. If the distance between the lane-changing vehicle and the preceding vehicle on the adjacent lane is too small, there may be a rear-end collision during lane change. In Fig. 8, when the spacing between Car B and Car C, denoted as d_1, is larger than d_{safe}, and the spacing between Car A and Car C, denoted as d_2, is larger than the limit gap d_0, the lane-changing condition is satisfied.

$$\begin{cases} d_1 > d_{safe} \\ d_2 > d_0, \end{cases} \quad where\ d_{safe} = v_i \cdot t_{desire} + d_0 \tag{17}$$

where d_{safe} is the minimum lane-changing spacing, v_i is the speed of the rear vehicle, t_{desire} is the expected headway of the lane-changing vehicle, and d_0 is the limit gap to ensure safe driving, typically ranging from 2 to 5 m, and is set to 5 m. Similar to the way of calculating expected speed, the expected headway $t_{desire-c} = 10.6$ s, $t_{desire-n} = 7.42$ s, and $t_{desire-a} = 6.3$ s. Spacing represents the spatial distance between the front and the rear vehicles, measured in meters.

C. Multi-Lane Game Model

In this part, a new multi-vehicle dynamic game mechanism is proposed to improve the Stackelberg Game theory, and an innovative game model named Multi-Lane Game Model is developed based on it.

Compared to traditional models, the Stackelberg game has asymmetric structure, which makes it better suited to real-world scenarios. Moreover, the clear sequence of actions

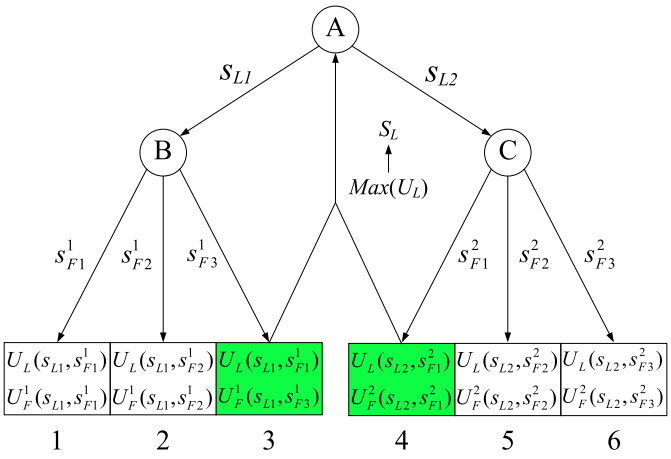

Fig. 9. The mechanism of Multi-Lane Game Model.

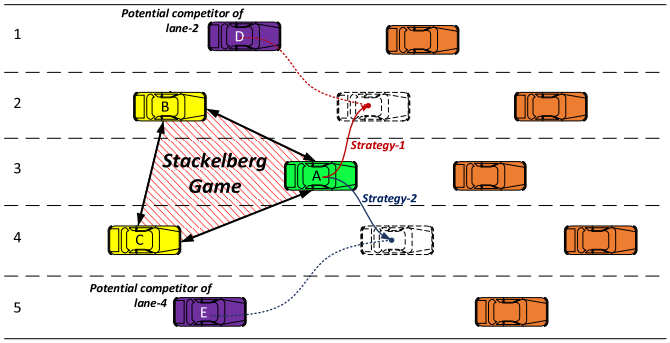

Fig. 10. The multi-vehicle game scenario.

improves both stability and computational efficiency. Therefore, the Stackelberg game is selected as the basis. In a Stackelberg game, participants are divided into a leader and followers, and the leader has more initiative. A complete game process can be summarized as the following steps: First, the leader assumes a decision, and followers will choose the optimal strategies to maximize their interests based on the leader's decision. After the leader assumes all situations in sequence, all possible outcomes are within his foresight. At the point, the leader makes the decision with the outcome that is most beneficial to himself. Finally, the followers can only make decisions as assumed by the leader, and otherwise, their benefits will be harmed. The entire game process is dynamic and asymmetric, and guided by the leader.

1) Design of New Multi-Vehicle Dynamic Game Mechanism: A new mechanism based on dynamic game paradigm is designed to improve the classical Stackelberg Game, and it is shown in Fig. 9, where each strategic combination produces a set of leader and follower payoff functions, yielding a total of six outcomes. The leader makes the final decision by anticipating the followers' responses to each possible decision. For example, if Car A decides to change into the left lane, Car B will slow down to maximize its payoff. And if Car A opts for the right lane, Car C will cruise for maximum payoff. Then, Car A only focuses on the two sets of payoff functions (numbered 3 and 4) and selects the strategy with the highest payoff for itself as its actual strategy. If crashes occur in both groups of strategies, it will give up lane change. Based on the mechanism, optimal strategies of the leader and followers are calculated by the following formulas. Fig. 10 is the scenario of the lane-changing game. After Car A makes a decision, either Car B or Car C makes the response, but not all players have to make decisions. If Car A's decision is changing into the left lane, only Car B needs to make the response. The actual players are determined in the middle of the game process, which breaks away from the structure of the classical game tree.

$$s_L^* = \arg\max\left(\max U_L\left(s_{Ln}, P\left(s_{Ln}\right)\right)\right) \tag{18}$$

$$s_F^{m^*} = \arg\max\left(\max U_F^m\left(s_L^*, s_F^m\right)\right)$$

$$s.t.\ m = \begin{cases} 1, & s_L^* = s_{L1} \\ 2, & s_L^* = s_{L2} \end{cases} \tag{19}$$

where s_L^* is the leader's optimal strategy, $s_F^{m^*}$ is the follower m's optimal strategy, s_{Ln} is the leader's any optional strategy, and $P(s_{Ln})$ represents the predicted action of a specific follower when the leader selects strategy s_{Ln}.

2) Construction of Multi-Lane Game Model: In Multi-Lane Game Model, the lane-changing vehicle plays as a leader and initiates the game. It makes decisions based on the driving information and style of both the rear vehicles and itself, while the followers make the optimal response based on the decision of the lane-changing vehicle. Under the background of intelligent transportation and IOV, a non-cooperative multi-vehicle game under complete information is constructed. As depicted in Fig. 10, the green car is the lane-changing vehicle, the orange cars are the preceding vehicles, the yellow cars are the rear vehicles participating in the game, and purple cars are potential competitors with intentions to change lanes. Define the three elements of Multi-Lane Game Model:

Players: All vehicles involved in the game. For example, in Fig. 10, players are Cars A, B, and C, where Car A is the leader while Car B and Car C are followers.

Strategies: Collections of all strategies that each participant can adopt individually. Define the leader's strategy set as S_L and $S_L = \{s_{L1}, s_{L2}\}$, where s_{L1} represents changing into the left lane and s_{L2} represents changing into the right lane. Define the strategy set of follower i as S_F^i and $S_F^i = \{S_{F1}^i, S_{F2}^i, S_{F3}^i\}$, where S_{F1}^i represents acceleration driving, S_{F2}^i represents cruising, and S_{F3}^i represents deceleration driving. The numbers i of the left and right followers are 1 and 2, respectively.

Payoffs: The leader's and followers' interests under specific strategic combinations. Define the leader's payoff funtion as U_L and $U_L = U_L(s_n, s_{Fk}^i)$ while the follower's payoff function is denoted as $U_F^i(s_n, s_{Fk}^i)$, where n and k are identifiers for the leader's and followers' strategies. Here, $n = 1, 2$ and $k = 1, 2, 3$.

3) Payoff Functions: The decisions of both the leader and followers are determined by the outcomes of payoff functions. Due to the distinctive concerns of the leader and followers in the game, their pursued goals have both commonalities and individual characteristics. For example, the leader needs to consider the conflicts and decide which lane to change into, while followers do not need to consider these

issues. Therefore, this paper designed payoff functions for the leader and followers respectively. It is worth noting that the short-term style obtained from the driving style classifier will be used in the design and calculation of various payoff functions, and the driving style of the ego lane-changing car will be used in the design of payoff weights.

a) Design of leader payoff function U_L:

$$U_L = \beta_1 U_p + \beta_2 U_{dL} - \beta_3 U_c \tag{20}$$

where β_1, β_2, β_3 are the weights of three payoff functions, and β_1, β_2 are determined by the driving style of the leader. If the style is aggressive, the vehicle will pay more attention to the increase of speed and the importance of spacing is reduced. After adjustments in repeated experiments, it is determined that (β_1, β_2) is (0.625, 0.375) for aggressive vehicles; (0.5, 0.5) for normal cars and (0.375, 0.625) for calm cars. This setting ensures that the weights of each payoff are differentiated and not overly biased. In case of a conflict, the leader should try to avoid lane-grabbing with competitors as much as possible, so the conflict payoff should significantly influence the total payoff, with $\beta_3 = 1$. Below, U_p, U_{dL}, and U_c will be introduced separately.

Potential payoff function U_p: The speed after the lane change is related to the lane-changing potential. Its definition and calculation have been detailed in part A.

$$U_p = R_q \tag{21}$$

Leader spacing payoff function U_{dL}: As the leader can predict followers' strategies by forseeing payoffs, the future state parameters of followers can be calculated as (22) to (24). After lane change, if the distance between the front and rear vehicles of the ego lane-changing vehicle is equal to the sum of leader's and follower's expected distances, the spacing payoff will be maximized, as shown in (25). If the spacing is equal to the minimum lane-changing gap d_{safe}, the payoff will be the smallest, as shown in (26), and if the spacing is less than d_{safe}, an accident will occur and the payoff value is set to negative infinity. Consequently, U_{dL} is calculated through (27).

$$v_i' = v_i + aT \tag{22}$$

$$x_i' = x_i + v_i T + 0.5 \cdot aT^2 \tag{23}$$

$$d_i' = x_{fi}' - x_i' \tag{24}$$

$$d_{iu\,\max}' = v_i' t_{i-desire} + v' t_{desire} \tag{25}$$

$$d_{iu\,\min}' = d_{safe} \tag{26}$$

$$U_{dL} = \begin{cases} 1, & d_i' > d_{iu\,\max}' \\ \dfrac{d_i' - d_{safe}}{d_{iu\,\max}' - d_{safe}}, & d_{iu\max}' \geq d_i' \geq d_{safe} \\ -\infty, & d_i' < d_{safe} \end{cases} \tag{27}$$

where i is lane number, and the left and right lane numbers are 1 and 2, respectively, a is the follower's acceleration determined by the decision, T represents the duration of lane changing, v_i' and d_i' represent the follower's speed and the distance from the original preceding vehicle after lane change, respectively, x_{fi}' represents the longitudinal position of the leader's preceding vehicle after lane change, and v' represents the leader's speed after lane change.

Lane-changing conflict payoff function U_c: In Fig. 10, if Car D or Car E intends to change into Car A's target lane at the same time, it will be a competitor. The higher the competitor's lane-changing demand and short-term style factor value, the lower the conflict payoff. A control factor Ψ is set to control whether the module is started. When there is a competitor, it is equal to 1; otherwise, 0. Lane-changing conflict payoff function U_c is expressed as shown in (28).

$$U_{ci} = \psi_i \cdot (R_{com} + \xi_s \cdot (s_{com} - 1)) \tag{28}$$

where R_{com} is the competitor's lane-changing demand, s_{com} is the competitor's short-term style factor, and ξ_s is the short-term style influencing factor.

b) Design of follower payoff function U_F:

$$U_F^i = \beta_4 U_{vi} + \beta_5 U_{dFi} \tag{29}$$

where β_4 and β_5 represent the weights of follower spacing payoff function U_{dF} and speed payoff function U_v. Similarly to (20), β_4 and β_5 are determined by the follower's driving style. (β_4, β_5) is (0.375, 0.625) for aggressive cars, (0.5, 0.5) for normal cars and (0.625, 0.375) for calm cars. Below, U_{dF} and U_v will be introduced.

Speed payoff function U_v:

$$U_{vi} = \begin{cases} \dfrac{v_i'}{v_{i-desire}}, & v_i' \leq v_{i-desire} \\ 1, & v_i' > v_{i-desire} \end{cases} \tag{30}$$

Follower spacing payoff function U_{dF}: After a lane change, the closer the distance between the follower and the leader is to the follower's expected spacing, the higher the resulting payoff. (31) defines the follower's expected spacing. When the spacing is greater than or equal to the expected spacing, the payoff is the largest, and when the spacing is the limit gap d_0, the payoff is the smallest. If the spacing is less than d_0, an accident will occur, and the payoff is negative infinity.

$$d_{i-desire} = v_{i-desire} \cdot t_{i-desire} \tag{31}$$

$$U_{dFi} = \begin{cases} 1, & d_{i-desire} \leq d_i'' \\ \dfrac{d_i'' - d_0}{d_{i-desire} - d_0}, & d_0 \leq d_i'' < d_{i-desire} \\ -\infty, & d_i'' < d_0 \end{cases} \tag{32}$$

where $i = 1$ and 2 represent the left and right followers, $d_{i-desire}$, $t_{i-desire}$ and $v_{i-desire}$ are the expected distance, headway, and speed of follower i, respectively, and d_i'' is the distance between the leader and the follower after a lane change.

c) Payoff space: Differing from payoff matrix in traditional game theory models, our model needs higher dimensional expression, and the payoff space is proposed. The input of the leader 's payoff function is a two-dimensional vector. Therefore, the leader's payoff has six possible results, while each follower's payoff has three possible results. In Fig. 11, Flat-1 and Flat-2 correspond to the leader's two decision branches, and each cuboid on flats represents the payoff result under a set of strategies.

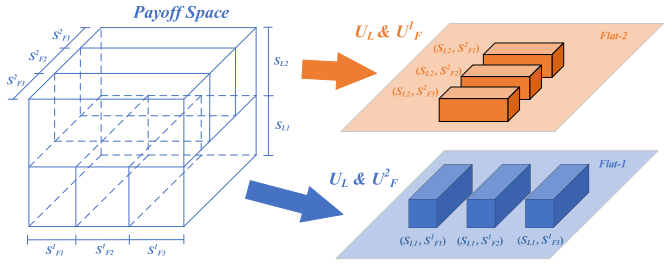

Fig. 11. Schematic diagram of the payoff space.

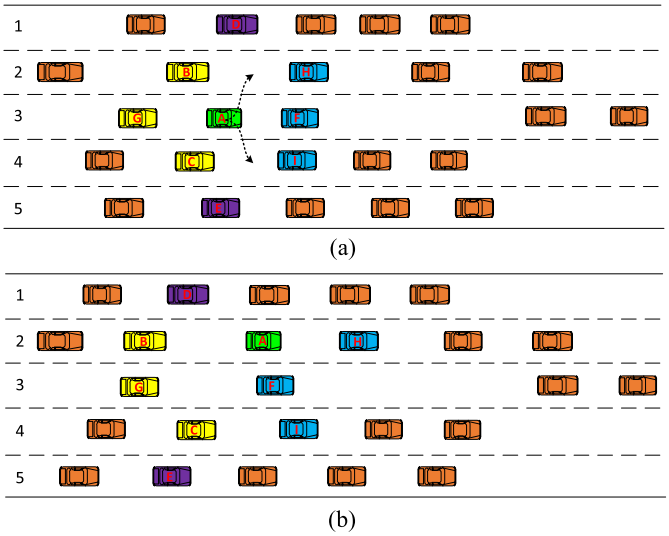

Fig. 12. A schematic diagram of the relative positions of all vehicles at the beginning and completion of the lane change. (a) Relative position status when Car A was about to change the lane (b) Relative position status when Car A had changed into Lane 2.

IV. Experiments and Result Analysis

We demonstrate the contributions of this paper through three experiments. Experiment A validates the overall effectiveness of the lane-changing model by analyzing the entire lane-changing process and the changes in various parameters; Experiment B validates the impact of incorporating traffic flow information into the model; and Experiment C validates the model's personalization and rationality by comparing its performance with that of human drivers.

Vehicle following in our experiments is managed by personalized adaptive cruise control (ACC) based on constant headway. ACC regulates longitudinal speed based on the expected headway, ensuring safety by increasing the following distance with rising speed. The vehicle executes the action of lane change through lateral and longitudinal decoupling speed control facilitated by a MPC controller.

A. Experiment A: Preceding Vehicle Abnormal Braking

1) Experimental Scenario and Parameter Settings: It is assumed that the experimental vehicles are intelligent connected vehicles. We build and test a five-lane scenario and track the state parameters (position, speed, spacing and headway) of five adjacent vehicles in each lane, totaling 25 vehicles. Parameters such as expected speed, headway, spacing of all vehicles are derived from the real data of NGSIM. The experiment introduces a scenario where Car F brakes abnormally at 150 s until its speed reaches 5 m/s. For generality, a lane-changing vehicle in Lane 3 is selected as the analysis object of the experiment. Fig. 12 is the schematic diagram of experimental scenario.

The lateral coordinate of the centerline of Lane 5 is set to 0 while the longitudinal coordinate of the last vehicle in Lane 3 is set to 0, and lane width is 3.5 m. Simulation duration is 300s and a single time step is 0.1s. Perception range of vehicles is 400m. Abnormal sensitivity factor threshold ε' is 0.2. The lane-changing demand threshold is 0.15 and duration threshold is 30s, which means that the vehicle starts changing lane when it is dissatisfied with the current driving conditions for 30 seconds. Overspeed loss coefficient α is set to 0.1 due to the minimal impact on lane-changing potential. In order to prevent excessive traffic fluctuations, the acceleration and deceleration of followers are set to 0.8m/s^2 and -0.8m/s^2. Considering that the impact of short-term style on payoff is far less than the lane-changing demand, the short-term style influence coefficient ξ_s is set to 0.1. In fact, these parameters can be set arbitrarily by the driver, and for example, aggressive drivers may set shorter duration thresholds and higher acceleration. The above settings are only a set of possible parameter values.

2) Analysis of the Results of Experiment A: Lane-changing demand for Cars A, D, and E are shown in Fig. 13 (a). Car A's demand exceeds the threshold at 162.7 s, so it changed into Lane 2 at 192.7 s, and the demand was cleared. After lane change, Car A was satisfied with the driving condition of Lane 2 and its demand value remained at 0. During the experiment, Cars D and E did not reach the threshold. Traffic flow speed and traffic anomaly coefficient of Car A's lane are shown in Fig. 13 (b). When Car F braked abnormally, the average speed of traffic flow decreased accordingly. After a period of time, the guide vehicle in Lane 3 left Car A's observation range, resulting in a sudden drop in average speed, as shown in the purple circle. Then Car A changed into Lane 2 and began to observe Lane 2's traffic flow, resulting in a sudden increase in speed, as shown in the green circle. The orange curve below illustrates that when Car F braked abnormally, the traffic anomaly coefficient increased rapidly and approached 1 gradually. Therefore, the calculation of Car A's lane-changing demand increasingly depended on its own speed rather than the traffic flow speed, preventing the traffic anomaly from interfering with Car A's decision-making. Now we analyze the process by data. After deceleration of Car F, the average traffic flow speed only slightly decreased to around 9 m/s, but Car A's demand increased to 0.28 rapidly and significantly. For comparison, the traffic flow speed of Lane5 was around 8 m/s but Car E's demand was only about 0.032. The phenomenon indicates that traffic anomaly coefficient ξ plays a crucial role in improving Car A's response speed to the traffic anomaly and compensates for the lack of traffic flow information.

The longitudinal speeds of Car A and the around Cars B, F, G, H are shown in Fig. 14 (a). Car A began to decelerated

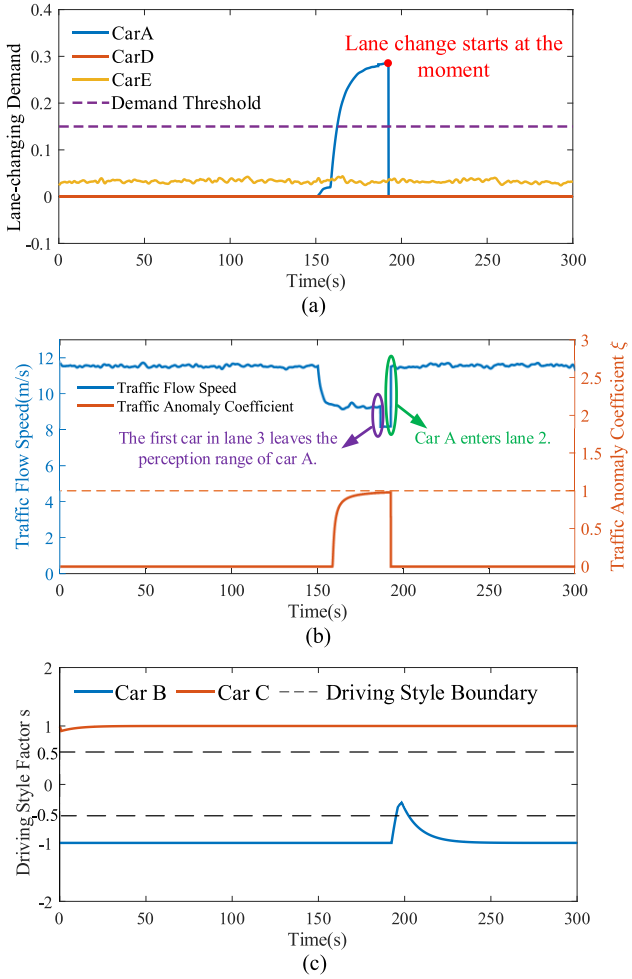

Fig. 13. Lane-changing demand, traffic flow speed and traffic anomaly coefficient, and short-term vehicle style. (a) lane-changing demand of Car A, D and E (b) Traffic flow speed and traffic anomaly coefficient (c) Short-term styles of Car B and Car C.

from 150 s and during lane change, the longitudinal speed of Car A quickly approached that of front Car H. After lane change, Car A adjusted its headway to the expected value through acceleration and then transitioned into a cruising state. Car B rapidly decelerated to 5m/s while Car A was changing the lane. At the completion of Car A's lane change, Car B rapidly accelerated to reduce the spacing and returned to cruise. Meanwhile, Car G accelerated to fill the gap left by Car A's departure.

Payoff results of the game are shown in Fig. 15. If Car A turns left, Car B will slow down to maximize its payoff, while if Car A turns right, Car C will cruise to maximize its payoff. Upon comparing these two sets of strategies, the "turn left" strategy will bring the most payoff to Car A, so it switches to Lane 2. At the same time, depending on the payoff results, Car B will definitely choose the deceleration strategy. Therefore, the game reaches an equilibrium state, and the equilibrium solution is (0.7074, 0.7718).

B. Experiment B: Traffic Flow Fluctuation

1) Experimental Scenario and Parameter Settings: This experiment mainly tests the performance of the system in the presence of speed fluctuations within the traffic flow. Speed curve of the guided vehicle in Lane 3 is depicted in Fig. 16. Lanes 1 and 5 are excluded from consideration in this experiment. To highlight the advantages of our system in stability and avoiding invalid lane changes, a contrast model is established. The model only changes the calculation based on traffic flow information to that based on the kinematic information of the single preceding vehicle, and the other contents are exactly the same as our system. To ensure the significance of comparison, the speeds of the guide vehicles in Lanes 2 and 4 are set to 5 m/s and 7 m/s. The threshold of lane-changing demand is set to 0.15, and the time threshold

TABLE IV
HUMAN DECISIONS VERSUS SYSTEM DECISIONS

Car ID	Human decisions	System decisions	Car ID	Human decisions	System decisions
39	L	L	791	L	L
60	**R**	**N**	**819**	**L**	**N**
81	R	R	828	L	L
96	L	L	838	R	R
362	R	R	848	R	R
405	L	L	857	R	R
425	L	L	860	L	L
432	L	L	**863**	**L**	**N**
445	R	R	906	L	L
468	L	L	917	L	L
492	L	L	946	L	L
526	**R**	**L**	947	R	R
555	L	L	1015	L	L
565	L	L	1019	L	L
567	**R**	**L**	**1031**	**R**	**L**
597	L	L	1109	L	L
598	**L**	**N**	1119	L	L
657	L	L	1302	L	L
665	L	L	1324	L	L
668	L	L	1456	L	L
697	L	L	1626	L	L
746	L	L	**1630**	**L**	**N**

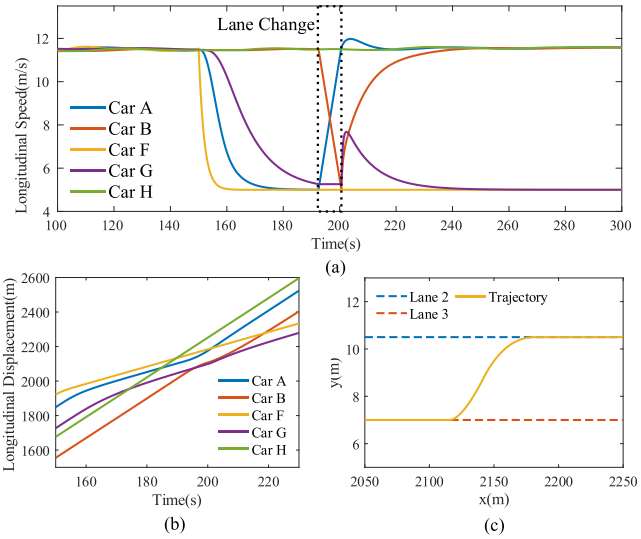

Fig. 14. Longitudinal speeds and displacements of relevant cars and the lane-changing trajectory of Car A. (a) The longitudinal speeds of the relevant cars (b) The longitudinal displacements of the relevant cars (c) The lane-changing trajectory of Car A.

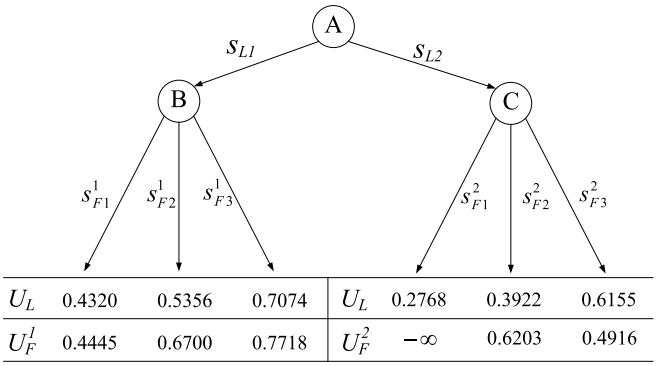

U_L	0.4320	0.5356	0.7074	U_L	0.2768	0.3922	0.6155
U_F^1	0.4445	0.6700	0.7718	U_F^2	$-\infty$	0.6203	0.4916

Fig. 15. Payoff results.

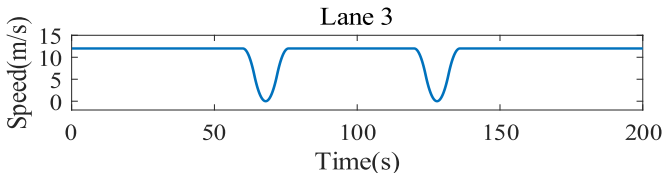

Fig. 16. The speed curve of the guiding vehicle in Lane 3.

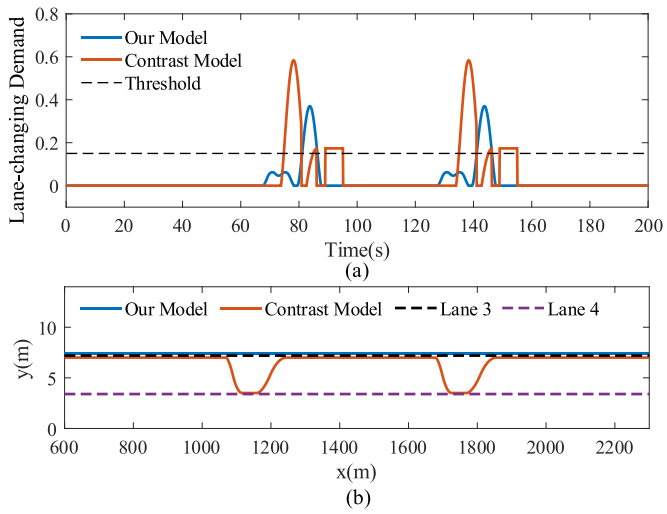

Fig. 17. Lane-changing demand and driving trajectories. (a) Comparison of the lane-changing demand between our model and the contrast model (b) Comparison of vehicle driving trajectories between our model and the contrast model.

is set to 6 s. All other settings are the same as Experiment A.

2) Analysis of the Results of Experiment B: As shown in Fig. 17 (a). The peak values of the lane-changing demands are 0.582 and 0.369, respectively. In the speed fluctuation, the durations of the two models exceeding the threshold are 13.2 s and 5.3 s, respectively. The maximum lane-changing demand of our model is 36.60% lower than that of contrast model, and the time exceeding the threshold is reduced by 59.84%. The lane-changing trajectory is shown in Fig. 17 (b). The vehicle with contrast model changed into Lane 4 due to dissatisfaction with following the preceding vehicle in Lane 3. However, when the traffic fluctuation in Lane 3 subsided, it returned to Lane 3 after another decision. Therefore, the two lane changes are invalid. When next fluctuation came, the vehicle again performed two invalid lane changes. In summary, our system avoids frequent and ineffective lane changes, which improves the driving comfort and the environmental performance. It also helps to reduce the safety risks associated with lane-changing maneuvers to some extent.

C. Experiment C: Comparison With Real Decisions

1) Experimental Scenario and Parameter Settings: This experiment compares the decisions made by our system with those made by human drivers. Among the 1124 vehicles, the vehicles that have changed lanes are of concern, and not only their IDs but also complete driving data of all vehicles within the perceptual range are required. After screening, 44 samples meet the requirements, and by restoring the driving scenarios, 44 sub-experiments are carried out. The time threshold is set to 10s through preliminary experiments on the samples and other parameters remain consistent with those in Experiment A.

2) Analysis of the Results of Experiment C: The comparison between real decisions and results of our model is presented in Table IV, where "L", "R" and "N" represent left, right, and no lane change, respectively. There are eight subtests in which our model makes different decisions. Inevitably, not all human drivers can make rational decisions, and in the eight tests, we will analyze in detail if the decisions made by our model are more rational.

It can be concluded from Table IV that among the eight tests, five tests have disagreements on the demand for lane change, and three on the decision of target lane. Cars 60, 598, 819, 863, and 1630 considered that there was no demand for lane change, while the views of human drivers were opposite. Upon analysis, it's found that these cars have not yet met the lane-changing demand threshold or have only briefly exceeded the threshold throughout the driving process. And from real data, we know that these vehicles did not increase speed or spacing after lane changes. Therefore, from a rational analysis, the lane-changing behaviors of human drivers did not bring a significant improvement in driving experience and were actually not worth doing. Compared with human drivers, Cars 526, 567, and 1031 made different decisions on target lanes. It's found that there is a commonality among the three human drivers: They excessively prioritize speed improvement, neglecting the spacing factor and exposing themselves to danger. In other words, the loss caused by reduction of spacing is higher than the benefit brought by speed increase. This may be due to the drivers' personality, mood and other factors. On the contrary, our model is not affected by the above factors and can make the highest-payoff decisions. In summary, our system successfully completed all experiments and consistently provided rational decisions, validating its safety and stability.

V. Conclusion

This paper proposes a lane-changing decision system which realizes multi-vehicle interactive lane change based on improved Stackelberg Game in multi-lane scenarios. The system consists of three parts: Lane-Changing

Demand Assessment, Lane-Changing Condition Assessment and Multi-Lane Game Model. Additionally, in order to personalize the system, an online driving style classifier is designed.

Lane-Changing Demand Assessment takes into account not only the driving data of the ego vehicle, but also 400-metre traffic flow information. It analyzes the urgency and potential of lane change to assess the demand, which enables the vehicle to rationally judge the necessity of lane change. Multi-Lane Game Model designs a multi-vehicle dynamic game mechanism to improve the classical Stackelberg Game theory. This mechanism enables lane-changing vehicles to determine actual players during the game process, effectively resolving the issue of lane change in multi-lane scenarios. Vehicles can fully consider the driving style of other vehicles and participate in the game according to their own preferences. Therefore, Multi-Lane Game Model addresses the current deficiencies in application of game theory in multi-lane lane change.

We designed three experiments to fully verify the performance of the proposed lane-changing decision system. In preceding vehicle abnormal braking experiment, the intelligence, effectiveness and reliability of our system are verified through analyzing relevant parameters. Traffic Flow Fluctuation Experiment demonstrates that our system can effectively improve stability of lane-changing demand and mitigate the issue of invalid lane changes resulting from excessive traffic fluctuations. Comparison with Real Decisions Experiment indicates that the decision-making of our system is more rational and reliable than that of human drivers, which can compensate for the defect that human drivers occasionally make irrational decisions.

In general, this paper improves the Stackelberg game model and broadens the application scope of game theory in the field of lane-change decision-making. Traditional game models face challenges in handling complex multi-lane scenarios, but the improved game model overcomes this limitation, providing a solution for future research on applying game theory to lane-changing decisions in multi-lane scenarios. Furthermore, the system proposed in this paper offers a new direction for future research: improving the underlying mechanism of game theory itself, rather than simply refining its functions.

REFERENCES

[1] K. Arai and S. Ray, "Spontaneous-braking and lane-changing effect on traffic congestion using cellular automata model applied to the two-lane traffic," *Int. J. Adv. Comput. Sci. Appl.*, vol. 3, no. 8, pp. 537–552, 2012.

[2] J. Ni, J. Han, and F. Dong, "Multivehicle cooperative lane change control strategy for intelligent connected vehicle," *J. Adv. Transp.*, vol. 2020, pp. 1–10, Feb. 2020.

[3] P. G. Gipps, "A model for the structure of lane-changing decisions," *Transp. Res. B, Methodol.*, vol. 20, no. 5, pp. 403–414, Oct. 1986.

[4] Q. Yang and H. N. Koutsopoulos, "A microscopic traffic simulator for evaluation of dynamic traffic management systems," *Transp. Res. C, Emerg. Technol.*, vol. 4, no. 3, pp. 113–129, Jun. 1996.

[5] P. Hidas, "Modelling lane changing and merging in microscopic traffic simulation," *Transp. Res. C, Emerg. Technol.*, vol. 10, nos. 5–6, pp. 351–371, Oct. 2002.

[6] T. Toledo, H. N. Koutsopoulos, and M. Ben-Akiva, "Integrated driving behavior modeling," *Transp. Res. C, Emerg. Technol.*, vol. 15, no. 2, pp. 96–112, Apr. 2007.

[7] D. Sun and L. Elefteriadou, "Lane-changing behavior on urban streets: An 'in-vehicle' field experiment-based study," *Comput.-Aided Civil Infrastruct. Eng.*, vol. 27, no. 7, pp. 525–542, Aug. 2012.

[8] Y. Hou, P. Edara, and C. Sun, "Modeling mandatory lane changing using Bayes classifier and decision trees," *IEEE Trans. Intell. Transp. Syst.*, vol. 15, no. 2, pp. 647–655, Apr. 2014.

[9] T. Toledo and R. Katz, "State dependence in lane-changing models," *Transp. Res. Rec., J. Transp. Res. Board*, vol. 2124, no. 1, pp. 81–88, Jan. 2009.

[10] N. Ding, X. Meng, W. Xia, D. Wu, L. Xu, and B. Chen, "Multivehicle coordinated lane change strategy in the roundabout under Internet of Vehicles based on game theory and cognitive computing," *IEEE Trans. Ind. Informat.*, vol. 16, no. 8, pp. 5435–5443, Aug. 2020.

[11] X. Mo, Y. Xing, and C. Lv, "Interaction-aware trajectory prediction of connected vehicles using CNN-LSTM networks," in *Proc. 46th Annu. Conf. IEEE Ind. Electron. Soc. (IECON)*, Singapore, Oct. 2020, pp. 5057–5062.

[12] D. Li and A. Liu, "Personalized lane change decision algorithm using deep reinforcement learning approach," *Appl. Intell.*, vol. 53, no. 11, pp. 13192–13205, Jun. 2023.

[13] S. Sharifzadeh, I. Chiotellis, R. Triebel, and D. Cremers, "Learning to drive using inverse reinforcement learning and deep Q-networks," 2016, *arXiv:1612.03653*.

[14] F. Ye, X. Cheng, P. Wang, C.-Y. Chan, and J. Zhang, "Automated lane change strategy using proximal policy optimization-based deep reinforcement learning," in *Proc. IEEE Intell. Vehicles Symp. (IV)*, Las Vegas, NV, USA, Oct. 2020, pp. 1746–1752.

[15] Y. Hou and P. Graf, "Decentralized cooperative lane changing at freeway weaving areas using multi-agent deep reinforcement learning," 2021, *arXiv:2110.08124*.

[16] J. Guo and I. Harmati, "Lane-changing system based on deep Q-learning with a request–respond mechanism," *Expert Syst. Appl.*, vol. 235, Jan. 2024, Art. no. 121242.

[17] Z. Zhou, Y. Wang, G. Zhou, K. Nam, Z. Ji, and C. Yin, "A twisted Gaussian risk model considering target vehicle longitudinal-lateral motion states for host vehicle trajectory planning," *IEEE Trans. Intell. Transp. Syst.*, vol. 24, no. 12, pp. 13685–13697, Dec. 2023.

[18] X. Liu, Y. Wang, K. Jiang, Z. Zhou, K. Nam, and C. Yin, "Interactive trajectory prediction using a driving risk map-integrated deep learning method for surrounding vehicles on highways," *IEEE Trans. Intell. Transp. Syst.*, vol. 23, no. 10, pp. 19076–19087, Oct. 2022.

[19] J. Lu, J. Li, Q. Yuan, and B. Chen, "A multi-vehicle cooperative routing method based on evolutionary game theory," in *Proc. IEEE Intell. Transp. Syst. Conf. (ITSC)*, Auckland, New Zealand, Oct. 2019, pp. 987–994.

[20] Z. Zhou, Y. Wang, R. Liu, C. Wei, H. Du, and C. Yin, "Short-term lateral behavior reasoning for target vehicles considering driver preview characteristic," *IEEE Trans. Intell. Transp. Syst.*, vol. 23, no. 8, pp. 11801–11810, Aug. 2022.

[21] H. Kita, K. Tanimoto, and K. Fukuyama, "A game theoretic analysis of merging-giveway interaction: A joint estimation model," in *Transportation and Traffic Theory in the 21st Century*, M. A. P. Taylor, Ed., Leeds, U.K.: Emerald Group Publishing, 2002, pp. 503–518.

[22] A. Talebpour, H. S. Mahmassani, and S. H. Hamdar, "Multiregime sequential risk-taking model of car-following behavior: Specification, calibration, and sensitivity analysis," *Transp. Res. Rec., J. Transp. Res. Board*, vol. 2260, no. 1, pp. 60–66, Jan. 2011.

[23] N. Smirnov, Y. Liu, A. Validi, W. Morales-Alvarez, and C. Olaverri-Monreal, "A game theory-based approach for modeling autonomous vehicle behavior in congested, urban lane-changing scenarios," *Sensors*, vol. 21, no. 4, p. 1523, Feb. 2021.

[24] M. Sun, Z. Chen, H. Li, and B. Fu, "Cooperative lane-changing strategy for intelligent vehicles," in *Proc. 40th Chin. Control Conf. (CCC)*, Shanghai, China, Jul. 2021, pp. 6022–6027.

[25] J. Yoo and R. Langari, "A predictive perception model and control strategy for collision-free autonomous driving," *IEEE Trans. Intell. Transp. Syst.*, vol. 20, no. 11, pp. 4078–4091, Nov. 2019.

[26] S. Pan, Y. Wang, and K. Wang, "A game theory-based model predictive controller for mandatory lane change of multiple vehicles," in *Proc. 4th CAA Int. Conf. Veh. Control Intell. (CVCI)*, Hangzhou, China, Dec. 2020, pp. 731–736.

[27] H. Yu, H. E. Tseng, and R. Langari, "A human-like game theory-based controller for automatic lane changing," *Transp. Res. C, Emerg. Technol.*, vol. 88, pp. 140–158, Mar. 2018.

[28] J. Guo and I. Harmati, "Lane-changing decision modelling in congested traffic with a game theory-based decomposition algorithm," *Eng. Appl. Artif. Intell.*, vol. 107, Jan. 2022, Art. no. 104530.

[29] Q. Zhang, R. Langari, H. E. Tseng, D. Filev, S. Szwabowski, and S. Coskun, "A game theoretic model predictive controller with aggressiveness estimation for mandatory lane change," *IEEE Trans. Intell. Vehicles*, vol. 5, no. 1, pp. 75–89, Mar. 2020.

[30] Z. Deng, W. Hu, Y. Yang, K. Cao, D. Cao, and A. Khajepour, "Lane change decision-making with active interactions in dense highway traffic: A Bayesian game approach," in *Proc. IEEE 25th Int. Conf. Intell. Transp. Syst. (ITSC)*, Macau, China, Oct. 2022, pp. 3290–3297.

[31] H. Zhao, "Design and implementation of an improved K-means clustering algorithm," *Mobile Inf. Syst.*, vol. 2022, pp. 1–10, Sep. 2022.

Tianluo Yao received the B.S. degree in vehicle engineering from Dalian University of Technology, Dalian, China, in 2022. He is currently pursuing the M.S. degree with the Department of Mechanical Engineering, Beijing Institute of Technology (BIT), Beijing, China. Since 2022, he has been with the Intelligent Vehicle Research Center, BIT. His research interests include lane-changing decision-making systems, and intelligent vehicle planning and control.

Hui Jin received the Ph.D. degree from the College of Automotive Engineering, Jilin University, Changchun, China, in 2001. He was a Post-Doctoral Researcher with the Department of Computer Science and Technology, Tsinghua University, Beijing, China. Since 2004, he has been an Associate Professor with the Department of Mechanical Engineering, Beijing Institute of Technology, Beijing. His current research interests include intelligent vehicle technology and vehicle dynamics control.